

# Model predictive current control method for four-leg three-level converter operating as shunt active power filter and grid connected inverter

K. ANTONIEWICZ\* and K. RAFAL

Institute of Heat Engineering, 21/25 Nowowiejska St., 00-665 Warsaw, Poland

**Abstract.** This paper presents model predictive control (MPC) with a finite control states set (FS) for three-level four-leg flying capacitor (FCC) converter. Principles of control method are presented and flying capacitor voltages control method is discussed. Experimental results of converter operating as a shunt active power filter (SAPF) and grid connected inverter (GCI) are shown.

**Key words:** multilevel converter, model predictive control (MPC), power quality.

## 1. Introduction

**1.1. Power electronics in modern power grids.** Power electronics play a crucial role in transformation of power systems into smart electrical energy networks commonly referred to as smart grids (SG). As shown in Fig. 1, major applications of power electronic converters include grid interfaces for renewable energy sources (RES), electric vehicles (EV) and a wide group of power quality conditioners (PQC) [1].

Most of modern RES, as well as EV chargers are connected to the grid via grid connected inverters (GCI), which are solely responsible for their cooperation with power system. GCI must operate under minimum current distortion even with highly distorted voltage and under grid fault conditions. Specifically, current control method directly influences power quality at the point of common coupling (PCC); the RES is connected to the public grid [2]. As a consequence of the constant development of RES, new challenges arise for the operation of SGs, as well as for creating new converter topologies and control methods [3].

On the other hand, the growing amount of industrial loads with non-linear behavior cause problems with electric power quality in distribution networks. Reactive and harmonic components reduce power factor and thus increase losses in the power system, as well as in customer transformers, installations and loads [4].

Non-linear loads, characterized by high current distortion, should be compensated by passive, active or hybrid harmonic filters [4]. Passive filters consist of LC resonant circuits tuned to provide low impedance path for specific harmonic components. It may be further extended with capacitors or inductors that compensate for reactive component of load current. In this

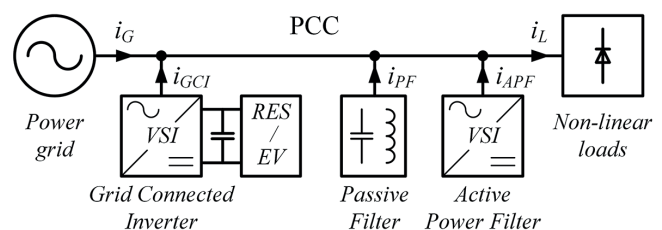


Fig. 1. Power electronics in smart grid

case non-active components of load current  $i_L$  are compensated by passive filter current  $i_{PF}$  and in an ideal case, grid current  $i_G$  remains sinusoidal with only active component.

Another way to achieve this goal is to install PQC, specifically, a converter-based shunt active power filter (SAPF). This solution includes a power electronic converter which is controlled to provide the compensation of harmonic and reactive components of load currents with the possibility of balancing phase currents in three-phase system [5]. This action requires a current control method to properly shape the compensation current [6].

Having GCIs operating with sinusoidal current and APF compensating non-linear loads, power grid can operate with sinusoidal currents, while reactive power flow can be compensated to zero or adjusted according to demand.

## 1.2. Current control methods for voltage source inverters.

One common feature of GCI and APF is that they typically employ a voltage source inverter (VSI) coupled to the power line by inductive filter. Over the years, many current control methods have been developed for voltage source converters [7].

A basic and the simplest solution is hysteresis controller. However, it introduces a variable switching frequency, which makes line filter design difficult. On the other hand, in a classical PI controller, a pulse width modulation (PWM) can be applied, but the dynamics will be limited by its period and

\*e-mail: antoniek@ee.pw.edu.pl

Manuscript submitted 2017-02-28, revised 2017-05-26, initially accepted for publication 2017-05-31, published in October 2017.

the frequency bandwidth of the PI controller. Although some methods to minimize effects of the above mentioned issues have been proposed (variable hysteresis bandwidth, feed-forward and feed-back loops), the process of control loop design is complicated, especially regarding the stability and tuning of controller parameters. Therefore, it is reasonable to adapt and develop other control strategies to find alternatives.

One of interesting options is model predictive control [8], which has been proposed and applied in the industry (e.g. chemical industry) about 50 years ago. This strategy employs the model of the controlled system to calculate the foreseen values of the state variables, regarding the available control states. Unfortunately, this quite simple idea can be computationally demanding, so for power electronics advanced control platforms are required (modern FPGA, DSP).

Among different types of MPC, the method based on a finite number of control states (FS-MPC) is chosen in this paper as a solution for power converter [8]. This method operates based on the assumption that in every sampling period, the system can only represent a finite number of states (switching states of the converter). FS-MPC offers high dynamics in transient states and an opportunity to extend, which makes it very suitable for current control applications, especially in multi-level converters [9–11].

**1.3. The scope of the paper.** This paper aims to implement FS-MPC control in a multilevel converter suitable for application in SGs. For this purpose, a four-leg three-level flying capacitor converter (FCC) topology is chosen. It was shown recently that in high power applications, three-level converters are an attractive alternative to two-level converters due to higher switching frequencies and lower filtering demands [12–13]. Particularly, for four-wire low voltage systems four-leg converters are preferred due to their inherent capabilities to operate under unbalanced and fault conditions [14].

In FCC topology, each converter leg contains an additional capacitor, called flying capacitor (FC). By a proper selection of the switching state, the capacitor can be connected in the circuit to generate an additional output voltage level. Therefore, capacitor voltages must be balanced to a proper level, which for three-level converter is half of the DC bus voltage. This operation is performed in each leg separately, which simplifies the control algorithm and makes FCC very suitable for multiphase applications.

The paper first shows a scheme of four-leg three-level FCC converter connected to the power grid. SAPF and GCI operations are discussed. Converter switching states and capacitor balancing method are presented. FS-MPC current control method is described with its principal formulas. Cost function is described and current reference generation methods are presented.

The described algorithm is confirmed with experimental results using 10 kVA laboratory system. Two important applications are considered:

- GCI – with a three-phase symmetrical, sinusoidal current reference examined under grid voltage distortions,
- SAPF – with a current reference set to compensate non-active components of load power.

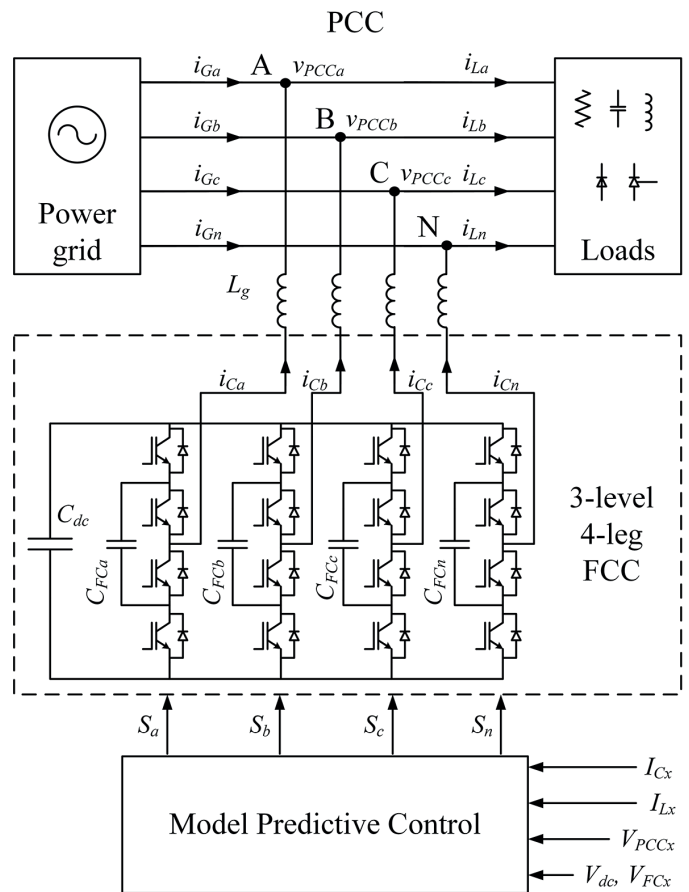


Fig. 2. Scheme of four-leg three-level FCC

## 2. Three-level four-leg converter

Figure 2 presents an overview of four-leg three-level FCC converter system. The converter is connected in parallel to the power grid in the PCC via L-type filter.

For operating as a SAPF, the converter currents  $i_{Cx}$  and non-linear load currents  $i_{Lx}$  are measured in the system (where  $x$  corresponds to  $a, b, c$  or  $n$  wire). The distortions introduced to the grid currents  $i_{Gx}$  by the load currents  $i_{Lx}$  are compensated by the currents  $i_{Cx}$  generated with SAPF, which can be expressed as:

$$i_{Gx}(t) = -i_{Cx}(t) + i_{Lx}(t), \quad (1)$$

Assuming the grid voltages symmetry, the grid neutral wire current  $i_{Gn} = 0$ , thus the load neutral wire current  $i_{Ln}$  should be fully compensated by  $i_{Cn}$ :

$$i_{Ln}(t) = -(i_{La}(t) + i_{Lb}(t) + i_{Lc}(t)), \quad (2)$$

$$i_{Cn}(t) = i_{Ln}(t), \quad (3)$$

$$i_{Gn}(t) = 0. \quad (4)$$

Expressions (1–4) can be considered as a mathematical description of a four-leg SAPF operation. The purpose of SAPF

is to properly control compensating current generated by converter, so that grid currents can be balanced and harmonic and reactive power components can be eliminated.

When operating as GCI, load current  $i_{Lx}$  is neglected in the scheme and system is simplified. Typically, a power source such as RES is connected to the DC bus of the converter and the converter delivers active power to the grid. However, this topology is also suitable to operate as an active rectifier. In this case grid current depends only on converter current:

$$i_{Gn}(t) = -i_{Ln}(t). \quad (5)$$

In general, the purpose of GCI operation is to maintain balanced, sinusoidal grid current, even if grid voltages are distorted [15].

### 3. Balancing capacitor voltages

A single leg of three-level FCC converter is shown in Fig. 3. Converter output voltages  $V_{Cx}$  are generated by proper choice of switching states in each converter leg. There are four possible transistor states combinations that do not result in a short circuit. State 0 results in connecting output terminal to the negative DC bus terminal, while state 2 connects output to the positive DC bus terminal. These states generate output voltage equal to 0 or  $V_{dc}$ , respectively.

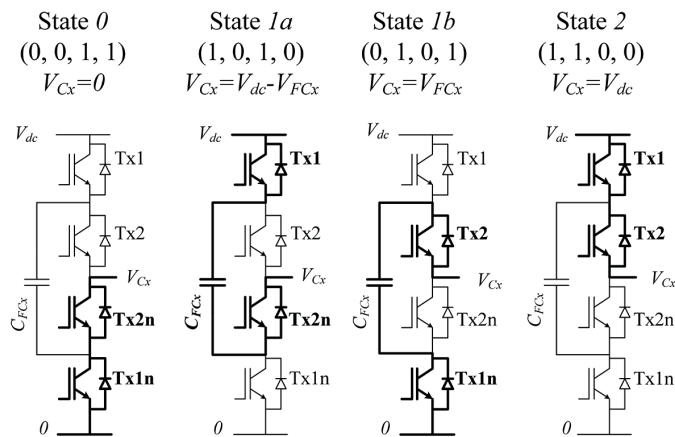


Fig. 3. Switching states of three-level FCC leg

In states 1a and 1b output voltage  $V_{Cx}$  depends on flying capacitor voltage  $V_{FCx}$ . It can be seen that if

$$V_{FCx}(t) = \frac{1}{2}V_{dc}, \quad (6)$$

output voltage for each state is the same and equals  $\frac{1}{2}V_{dc}$ . Therefore, fulfilling (6) is essential for symmetrical, three-level operation of FCC converter leg. Under this condition states 1a and 1b can be treated as redundant from the current control point of view, which greatly simplifies the synthesis of FS-MPC algorithm [16].

However, during converter operation FC charge is modified in states 1a and 1b by converter current  $i_{Cx}$  that flows through FCs. This results in a necessity of constantly controlling FC voltages. This is accomplished by the proper choice of redundant switching states that result in a change of direction of  $i_{Cx}$  current flow through FC. Principles for choice of switching states leading to FC voltage balancing are summarized in Table 1.

Table 1  
Flying capacitor voltage balancing principles

System state	Next switching state
$(i_{Cx} \geq 0)$ and $(V_{FCx} \geq V_{dc}/2)$	1b
$(i_{Cx} < 0)$ and $(V_{FCx} < V_{dc}/2)$	
$(i_{Cx} \geq 0)$ and $(V_{FCx} < V_{dc}/2)$	1a
$(i_{Cx} < 0)$ and $(V_{FCx} \geq V_{dc}/2)$	

In the proposed scheme, the control of FCs voltages is implemented outside the MPC loop. An additional function realizes the conditions gathered in Table 1 and selects the preferable state for each leg. Thus the system model is simplified and the amount of calculations is reduced. Another advantage of FCC converter is that capacitor balancing can be conducted for each leg separately, which simplifies control design.

Note that in the case of three-level neutral point clamped (NPC) converter capacitor, voltage balancing is much different, as all of the converter legs share the same DC bus with split capacitor bank. The task of voltage balancing algorithm is to split voltage equally between capacitors; it involves the consideration of current in all legs. Successful experiments regarding such balancing method have been reported in [17].

### 4. Model predictive control

MPC became an interesting alternative to classical methods based on PI or hysteresis controllers, while it is able to eliminate the disadvantages of aforementioned. It is very dynamic, gives suitable and optimal response to system state (PI has limited bandwidth) and can handle the control of several state variables (current, voltage, etc.) with one function, called cost function.

Block scheme of MPC applied to FCC converter is presented in Fig. 4. Two fundamental issues concern the developing a predictive model of the system and defining the cost function, which determines the aim of control.

According to [8], depending on the system functionality (rectifier, inverter etc.), different types of model can be used. Considering a model of a single leg or wire of the presented device, a discrete equation (at the basis of Kirchhoff's law) is given as follows:

$$L_g \frac{(i_{Cx}(k) - (i_{Cx}(k-1)))}{\Delta T_s} + R_g i_{Cx}(k) + S_m(k) V_{dc} = \quad (7)$$

$$= v_{PCx}(k) + v_{nN}(k).$$

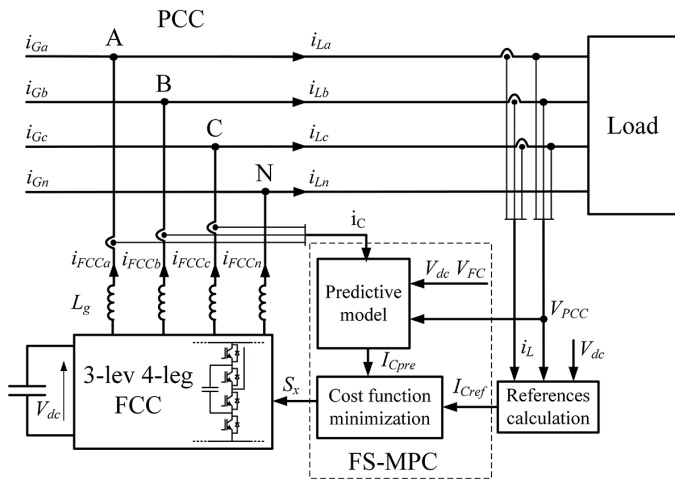


Fig. 4. FS-MPC control scheme

After transformation the equation can be rewritten as:

$$i_{pre,yx}(k+1) = \frac{T_s}{R_g T_s + L_g} [V_{dc}(S_y - S_x) - (v_{PCCy}(k+1) - v_{PCCx}(k+1))] + (8) + \frac{L_g}{R_g T_s + L_g} [i_{Cy}(k) - i_{Cx}(k)]$$

where:  $k$  – actual sampling step of control;  $i_{pre}$  and  $i_C$  – predicted and measured FCC currents respectively;  $T_s$  – sampling time;  $V_{dc}$  – DC bus voltage;  $v_{PCC}$  – grid voltage at PCC (for leg  $n$ , the voltage  $v_{PCCn}$  equals zero);  $v_{nN}$  – voltage between FCC DC negative bus and grid neutral wire;  $S_x$  – switching state in corresponding FCC converter leg;  $L_g$  and  $R_g$  – inductance and resistance of the passive filter, index  $y$ , similarly to  $x$ , corresponds to legs  $a, b, c$  or  $n$  ( $x \neq y$ ) of the FCC.

Although  $u_{nN}$  is possible to calculate, it depends on the switching states  $S$  in all legs, which increases the amount of calculations at the prediction stage. To reduce calculations a wire-to-wire model is used, giving the prediction equation [18] in the following form (assuming  $R_g = 0$ ):

$$i_{pre,yx}(k+1) = \frac{T_s}{L_g} [V_{dc}(S_y(k+1) - S_x(k+1)) - (v_{PCCy}(k) - v_{PCCx}(k))] + (9) + [i_{Cy}(k) - i_{Cx}(k)].$$

As can be seen, all currents and switching states of the FCC converter can be included in the control loop. Equation (9) can be based on phase voltages, giving currents  $i_{pre,yn}$  ( $y \in (a, b, c)$ ) and, additionally, on line voltages, giving currents  $i_{pre,yx}$  ( $x, y \in (a, b, c), x \neq y$ ) to improve the control of phase currents.

The measured values of compensation currents  $i_C$ , grid voltages  $V_{PCC}$ , DC-capacitor voltage  $V_{dc}$  and the considered control (switching) state  $S$  are used in (9) to predict the values of the converter currents  $i_{pre,yx}$  in the forthcoming sampling period. Errors are summarized in the cost function:

$$J(S_{abcn}(k+1)) = w_{f1} \sum_{y=a,b,c} abs(i_{Cref,yn}(k+1) - i_{pre,yn}(k+1)) (10) + w_{f2} \sum_{x,y=a,b,c,n} abs(i_{Cref,yx}(k+1) - i_{pre,yx}(k+1)).$$

Cost function must take into account a finite set (FS) of converter switching states, which is defined by the number of available switching states of three-level four-leg FCC. An overall number equals  $4^4 = 256$ . However, remembering that each leg has two redundant states  $1a$  and  $1b$ , generating the same output voltage level (see Fig. 2), they can be considered as one state  $1$ . This way the number of states will be reduced to  $3^4 = 81$  [1], which is much more affordable.

Finally, all cost function values are compared, to select the state  $S$ , for which  $J$  obtained the minimum. States are set for a whole sampling period, what induces an issue of variable switching frequency. However, there are several methods to reduce frequency variations, like those presented in [19].

The last task of the control algorithm – generation of reference currents – is performed outside FS-MPC algorithm. Generation of reference currents  $i_{Cref}$  depends on converter operation mode. For SAPF, case current references calculation is based on instantaneous power theory [20, 21]. For GCI, balanced sinusoidal currents are set as a reference.

## 5. Experimental results

The proposed FS-MPC method was validated experimentally on the laboratory model. For SAPF operation, experimental setup reflects the scheme shown in Fig. 2. In GCI mode, load model is removed and DC source is connected to the DC bus of the converter. Block schemes of experimental setup for both modes are shown in Fig. 5.

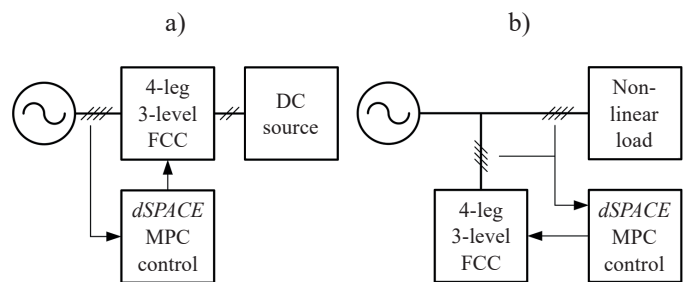


Fig. 5. Block scheme of experimental system in: a) GCI mode, b) SAPF mode

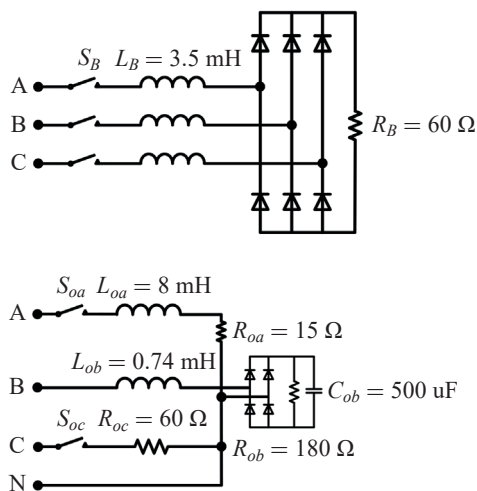


Fig. 6. Non-linear load model

Converter is controlled by control platform dSPACE1006mp. Parameters of experimental system are listed in Table 2. Presented waveforms were captured with Tektronix DPO5104B and TDS5034B digital oscilloscopes and displayed with Matlab.

Table 2  
Experimental system parameters

Parameter	Value
Converter power rating	10 kVA
Grid voltage $V_g$	230 V
DC bus voltage $V_{dc}$	700 V
DC bus capacitance $C_{dc}$	1.5 mF
FC capacitance $C_{FC}$	250 \$\mu\$F
Grid filter inductance $L_g$	1.5 mH
Sampling frequency $f_s$	30 kHz

It must also be mentioned that there was a significant operational delay of employed control platform, mainly due to handling of ADC, which, in the research, took up to 28 \$\mu\$s. The control uses prediction equation to compensate the delay based on stored data.

First, operation of converter controlled with FS-MPC method was examined in SAPF operation mode. The system was operated with unbalanced non-linear load, composed of circuits shown in Fig. 6 operating in parallel.

Figure 7 illustrates FS-MPC performance during two transients. The results are divided into three sections. In the first all switches in the load circuit are opened, so only phase B (see Fig. 5) of asymmetrical load is connected. In the second, phases A and C of that load are connected at 0.045 s. Finally, a three-phase bridge is connected at 0.195 s. As can be seen, the distortions introduced by the load currents are compensated by

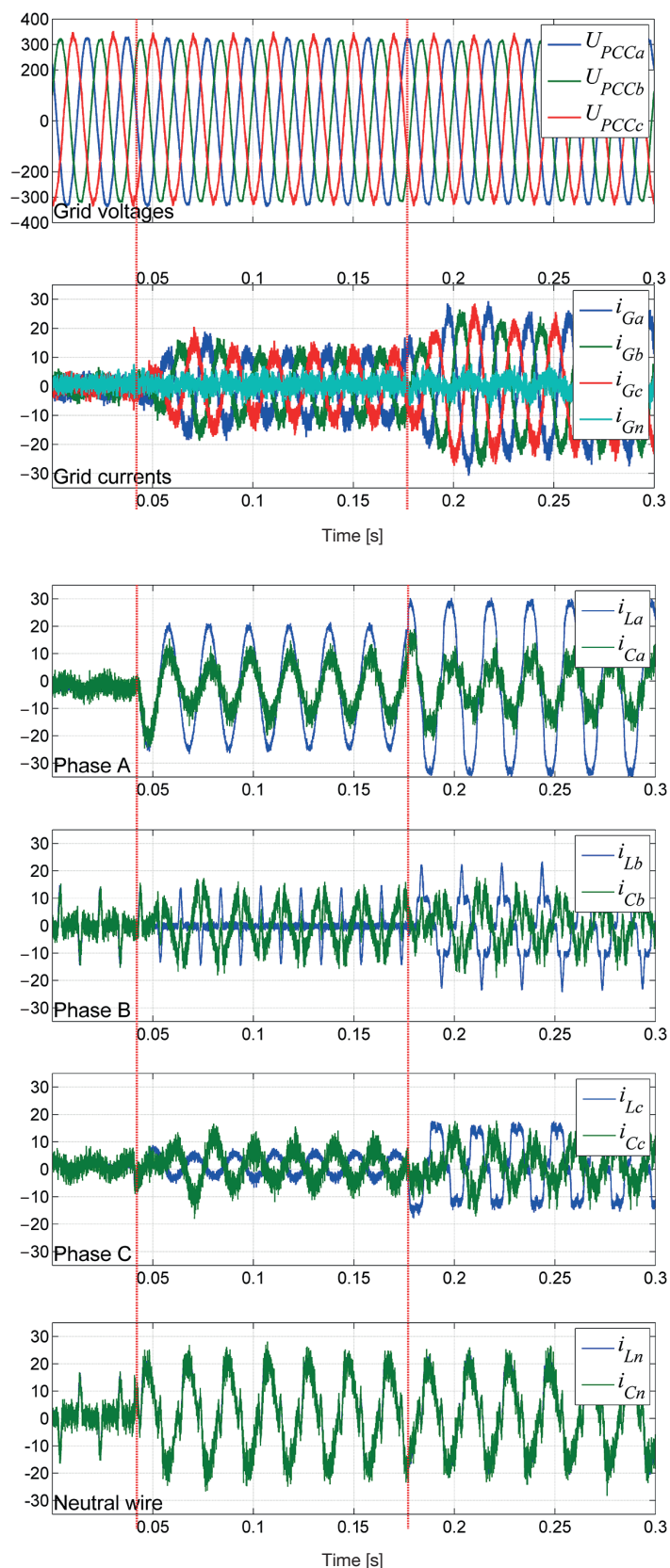


Fig. 7. The performance of FS-MPC in two transient states. From the top, first plot – grid voltages  $U_{Ga}$ ,  $U_{Gb}$ ,  $U_{Gc}$ , second plot – grid currents  $i_{Ga}$ ,  $i_{Gb}$ ,  $i_{Gc}$ , 3-rd to 6-th plot – load currents  $i_{La}$ ,  $i_{Lb}$ ,  $i_{Lc}$ ,  $i_{Ln}$ , compared in pairs with respective compensation current:  $i_{Ca}$ ,  $i_{Cb}$ ,  $i_{Cc}$ ,  $i_{Cn}$

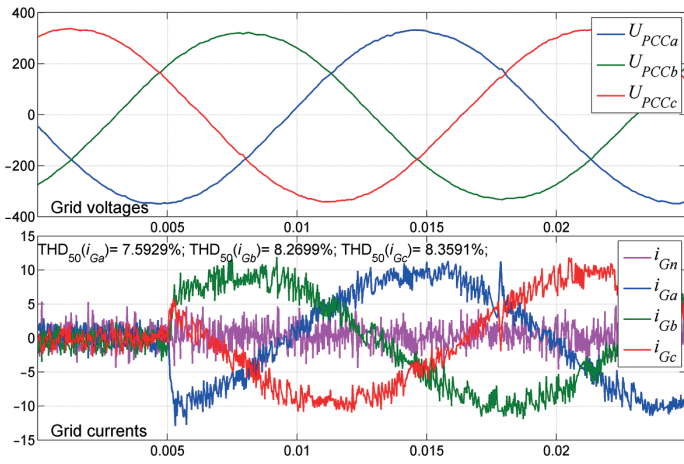


Fig. 8. Operation of GCI in dynamic state: step change of referenced active current from 0 to 10 A. On the top grid voltages; bottom: grid currents

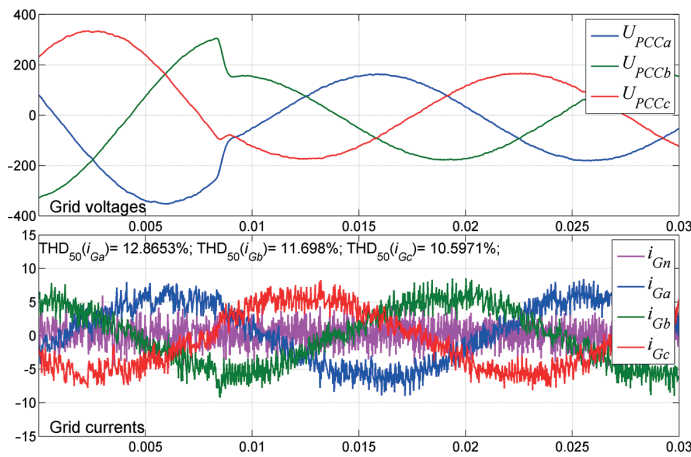


Fig. 9. Operation of GCI in dynamic state: 50% voltage dip with constant reference current amplitude 6 A. On the top grid voltages; bottom: grid currents

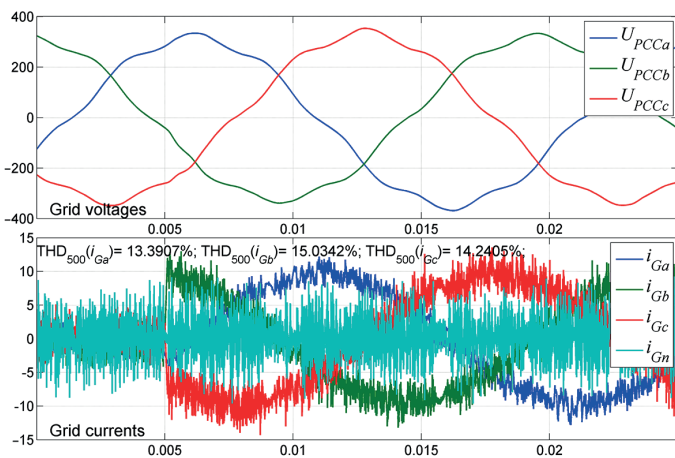


Fig. 10. Operation of GCI in steady state under 5% of 7<sup>th</sup> harmonic grid voltages distortion; top: grid voltages, bottom: grid currents

the generated FCC-SAPF currents. The resulting grid currents are sinusoidal and in phase with phase voltages. More results of SAPF operation can be found in [22].

The operation of converter in GCI mode is presented in Figs. 8–10. Note that value of grid filter is relatively low and results in high amplitude of grid current ripples.

Transient response illustrating step change in reference current amplitude from 0 to 10 A is shown in Fig. 8. It is demonstrated that the dynamics of MPC current control is very high, close to  $di/dt$  limit imposed by grid filter  $L_g$ . Figure 9 shows transient response to the disturbance (50%, three-phase grid voltage dip). The control algorithm responds within single sampling cycles, making current disturbance hardly noticeable.

Finally, algorithm resistivity to periodic disturbance such as higher harmonic is verified. Figure 10 presents converter operation under grid voltage disturbed by (5% of 7<sup>th</sup> harmonic content). It is shown that FS-MPC algorithm operate with dynamics sufficient to compensate for harmonic voltage disturbances without any additional control loops.

Note that proper operation of power converters operated under model predictive control methods relies on proper identification of physical model parameters. Parameter mismatch can lead to prediction error, which results in increased steady state errors and degenerated dynamic behavior [23]. Detailed analysis of this phenomenon is out of the scope of this paper and will be presented in further works.

## 6. Summary and conclusions

A model predictive control with finite states (FS-MPC) applied to four-leg three-level flying capacitor converter (FCC) was described in this paper. The method of flying capacitor (FC) voltages balancing was also discussed.

Viability of proposed method has been confirmed with experimental results of a 10 kVA system. Results include operation of converter a shunt active power filter (SAPF) and grid connected inverter (GCI). Steady-state and transient operation was considered, exposing designed control algorithm to step and harmonic changes of reference current as well as distortions in grid voltage.

Based on presented experimental results, the following conclusions are drawn.

- Four-leg three-level FCC is a viable solution for operation with unbalanced currents and voltages.
- Flying capacitors (FCs) voltages control was operated effectively in both SAPF and GCI operation, achieving balanced FCs' voltages.
- Due to independent FC voltage control in each leg, voltage balancing algorithm is simplified and operates effectively under unbalanced and distorted currents.
- FS-MPC assures fast and accurate current control in both SAPF and GCI operation modes.
- Using wire-to-wire equations of the SAPF model, prediction equations were simplified; currents prediction loop can employ the developed model in different ways, giving phase-to-neutral or phase-to-phase currents, etc.

- FS-MPC presents superb immunity to grid voltage disturbances, providing proper current control under grid voltage disturbances such as higher harmonics and voltage dips.
- FS-MPC is able to compensate existing operational delays of the control platform, which was meaningful for the prediction loop and switching state selection.

**Acknowledgements.** The project was financed with National Science Center funds based on decision no. DEC-2013/09/B/ST7/01608.

## REFERENCES

- [1] R. Strzelecki and G. Benysek, *Power Electronics in Smart Electrical Energy Networks*, Springer, 2008.
- [2] H. Abu-Rub, M. Malinowski, and K. Al-Haddad, *Power Electronics for Renewable Energy Systems, Transportation and Industrial Applications*, John Wiley & Sons, Ltd, 2014.
- [3] R. Teodorescu, M. Liserre, and P. Rodriguez, *Grid Converters for Photovoltaic and Wind Power Systems*, John Wiley & Sons, Ltd, 2011.
- [4] K. Rafał and M.P. Kaźmierkowski, “Sterowanie układem STATCOM z zasobnikiem energii z kompensacją wyższych harmonicznych i symetryzacją napięć”, *Przegląd Elektrotechniczny* 88 (12A), 1–5 (2012), [in Polish].
- [5] H. Akagi, “Modern active filters and traditional passive filters”, *Bull. Pol. Ac.: Tech.* 54 (3), 255–269 (2006).
- [6] T. Orłowska-Kowalska, F. Blaabjerg, and J. Rodriguez, *Advanced and Intelligent Control in Power Electronics and Drives*, Springer, 2014.
- [7] M.P. Kaźmierkowski and L. Malesani, “Current control techniques for three-phase voltage-source PWM converters: a survey”, *IEEE Trans. Ind. Electron.* 45 (5), 691–703 (1998).
- [8] J. Rodriguez and P. Cortes, *Predictive Control of Power Converters and Electrical Drives*, Wiley-IEEE Press, 2012.
- [9] J. Rodriguez et al., “State of the art of finite control set model predictive control in power electronics”, *IEEE Trans. Ind. Informatics*, 9 (2), 1003–1016 (2013).
- [10] P. Wiatr and M.P. Kaźmierkowski, “Model predictive control of multilevel cascaded converter with boosting capability – a simulation study”, *Bull. Pol. Ac.: Tech.* 64 (3), 581–590 (2016).
- [11] T. Geyer and D.E. Quevedo, “Performance of multistep finite control set model predictive control for power electronics”, *IEEE Trans. Power Electron.* 30 (3), 1633–1644 (2015).
- [12] R. Teichmann, M. Malinowski, and S. Bernet, “Evaluation of three-level rectifiers for low-voltage utility applications”, *IEEE Trans. Ind. Electron.* 52 (2), 471–481 (2005).
- [13] J. Rodriguez et al., “Multilevel converters: An enabling technology for high-power applications”, *Proc. IEEE* 97 (11), 1786–1817 (2009).
- [14] M. Sedlak, S. Styński, M.P. Kaźmierkowski, and M. Malinowski, “Operation of four-leg three-level flying capacitor grid-connected converter for RES”, *Proc. IEEE IECON* 39, 1100–1105 (2013).
- [15] M. Bobrowska-Rafał, K. Rafał, G. Abad, and M. Jasiński, “Control of PWM rectifier under grid voltage dips”, *Bull. Pol. Ac.: Tech.* 57 (4), 337–343 (2009).
- [16] F. Defay, A.-M. Llor, and M. Fadel, “A predictive control with flying capacitor balancing of a multicell active power filter”, *IEEE Trans. Ind. Electron.* 55 (9), 3212–3220 (2008).
- [17] V. Yaramasu, M. Rivera, M. Narimani, B. Wu, and J. Rodriguez, “Finite state model-based predictive current control with twostep horizon for four-leg NPC converters”, *J. Power Electron.* 14 (6), 1178–1181, (2014).
- [18] P. Acuna, L. Moran, M. Rivera, J. Dixon, and J. Rodriguez, “Improved active power filter performance for renewable power generation systems”, *IEEE Trans. Power Electron.* 29 (2), 687–694 (2014).
- [19] J. Rodriguez et al., “Predictive current control of a voltage source inverter”, *IEEE Trans. Ind. Electron.* 54 (1), 495–503 (2007).
- [20] K. Antoniewicz, M. Jasiński, M. Kaźmierkowski, and M. Malinowski, “Model predictive control for three-level four-leg flying capacitor converter operating as shunt active power filter”, *IEEE Trans. Ind. Electron.* 63 (8), 5255–5262 (2016).
- [21] H. Akagi, E.H. Watanabe, and M. Aredes, *Instantaneous Power Theory and Applications to Power Conditioning*, IEEE Press-Wiley, 2007.
- [22] K. Antoniewicz, M. Jasiński, M. Kaźmierkowski, and M. Malinowski, “Model predictive control for three-level four-leg flying capacitor converter operating as shunt active power filter”, *IEEE Trans. Ind. Electron.* 63 (8), 5255–5262 (2016).
- [23] H.A. Young, M.A. Perez, and J. Rodriguez, “Analysis of finite-control-set model predictive current control with model parameter mismatch in a three-phase inverter”, *IEEE Trans. Ind. Electron.* 63 (5), 3100–3107 (2016).